NeuroImage 118 (2015) 456–467

Contents lists available at ScienceDirect

NeuroImage

journal homepage: www.elsevier.com/locate/ynimg

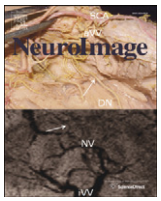

Effects of lesions on synchrony and metastability in cortical networks

František Váša [a,b,*,1], Murray Shanahan [b], Peter J. Hellyer [a,c], Gregory Scott [a], Joana Cabral [d], Robert Leech [a]

[a] Computational, Cognitive & Clinical Neuroimaging Laboratory, Department of Medicine, Imperial College London, London, UK
[b] Department of Computing, Imperial College London, London, UK
[c] Centre for Neuroimaging Sciences, Institute of Psychiatry, King's College London, UK
[d] Department of Psychiatry, University of Oxford, Oxford, UK

ARTICLE INFO

Article history:
Received 10 April 2015
Accepted 15 May 2015
Available online 3 June 2015

Keywords:
Neural dynamics
Kuramoto model
Metastability
Connectome
Graph theory
Stroke

ABSTRACT

At the macroscopic scale, the human brain can be described as a complex network of white matter tracts integrating grey matter assemblies — the human connectome. The structure of the connectome, which is often described using graph theoretic approaches, can be used to model macroscopic brain function at low computational cost. Here, we use the Kuramoto model of coupled oscillators with time-delays, calibrated with respect to empirical functional MRI data, to study the relation between the structure of the connectome and two aspects of functional brain dynamics — synchrony, a measure of general coherence, and metastability, a measure of dynamical flexibility. Specifically, we investigate the relationship between the local structure of the connectome, quantified using graph theory, and the synchrony and metastability of the model's dynamics. By removing individual nodes and all of their connections from the model, we study the effect of lesions on both global and local dynamics. Of the nine nodal graph-theoretical properties tested, two were able to predict effects of node lesion on the global dynamics. The removal of nodes with high eigenvector centrality leads to decreases in global synchrony and increases in global metastability, as does the removal of hub nodes joining topologically segregated network modules. At the level of local dynamics in the neighbourhood of the lesioned node, structural properties of the lesioned nodes hold more predictive power, as five nodal graph theoretical measures are related to changes in local dynamics following node lesions. We discuss these results in the context of empirical studies of stroke and functional brain dynamics.

Introduction

The ensemble of macroscopic white matter brain connections can be described as a complex network, the structural connectome, consisting of nodes corresponding to grey matter assemblies and edges, or connections, corresponding to structural white matter pathways between them (Hagmann, 2005; Sporns et al., 2005). Besides enabling a holistic characterization of the brain's architecture, the structural connectome, combined with a suitable model, enables the simulation of whole-brain dynamics at low computational cost (Honey et al., 2009). Simulated time-courses can then be compared to empirical functional data (Honey et al., 2009; Cabral et al., 2011; Deco et al., 2013) or analyzed using mathematical tools from dynamical systems theory, to quantify properties such as entropy or synchrony of the simulated neural activity (Honey and Sporns, 2008; Shanahan, 2010).

A notable application of such tools concerns the stability of brain dynamics. Within the brain, communication between neural ensembles is hypothesized to occur through coherence, whereby two neural assemblies whose activity fluctuates in synchrony can exchange information (Fries, 2005). However, a consistently coherent, stable state would be pathological. Thus, for efficient, flexible communication, variability of coherence is equally important. Accordingly, the healthy brain exhibits features of *multistability*, comprising multiple stable states but requiring external input to shift between them (Friston, 2001; Ashwin et al., 2007; Freyer et al., 2011, 2012) as well as *metastability*, spontaneously shifting between transient attractor-like states (Kelso, 2012; Shanahan, 2010; Tognoli and Kelso, 2014).

The notion of metastability is highly relevant to brain activity, which even in the so-called "resting-state" is a dynamic process. The brain in the absence of a specific task, alternating between temporarily stable states, has been compared to a tennis player, hopping on their two feet in preparation to hit the ball regardless of its incident direction (Deco et al., 2009). Besides providing a fast response to any stimulus, resting-state dynamics have been hypothesized to consolidate past events and stabilize neural ensembles (Buckner and Vincent, 2007). Whilst the relevance of metastable processes to cognition is beginning to be directly addressed (Deco et al., 2013; Hellyer et al., 2014), and a

* Corresponding author at: Brain Mapping Unit, Department of Psychiatry, Sir William Hardy Building, Downing Street, Cambridge CB2 3EB, UK.
E-mail address: fv247@cam.ac.uk (F. Váša).
[1] Present address: Brain Mapping Unit, Department of Psychiatry, University of Cambridge, Cambridge, UK.

http://dx.doi.org/10.1016/j.neuroimage.2015.05.042

link between the metastability of brain dynamics and slow cortical oscillations has been drawn (Cabral et al., 2011; Cabral et al., 2014a), the relationship between the structure of the brain and the metastability of its dynamics has not been systematically investigated.

Lesion studies have shed light on our understanding of brain networks. For example, they have been used to study the structural robustness of cortical networks (Hagmann et al., 2007; Kaiser et al., 2007) and to identify the core white matter scaffold of the human brain (Irimia and Van Horn, 2014). Moreover, lesion studies have previously been used to understand the effects of local structural organization on network dynamics, demonstrating the integrative role of "connector" hubs in the macaque brain (Honey and Sporns, 2008), relating the graph theoretical properties of the lesioned regions to disparity between simulated and empirical neural dynamics (Alstott et al., 2009) and paralleling empirical results of functional connectivity in schizophrenia patients (Cabral et al., 2012). However, the effect of lesions on synchrony and metastability in the human brain has not yet been investigated.

Here, we combine a calibrated model of human functional connectivity constrained by the white matter connectome with a focal lesioning approach to investigate the relationship between structural connectivity of macroscopic brain regions and large-scale neural dynamics. Our computational model is based on a network of Kuramoto oscillators (Kuramoto, 1984), coupled according to a 66 region of interest (ROI) cortical connectome (Hagmann et al., 2008) and incorporating delays determined by the lengths of the corresponding anatomical white-matter tracts. We first tuned the model to resemble empirical resting-state cortical dynamics by evaluating a two-dimensional parameter space, scaling the coupling strength and delay of oscillator interactions. For each of the dynamical regimes generated by this search, we evaluated the fit of the model to empirical functional connectivity derived from functional magnetic resonance imaging (fMRI), using both time-averaged functional connectivity and intrinsic connectivity networks (ICNs) extracted using independent component analysis (ICA). We then explored the importance of individual network nodes in determining functional dynamics, using a repeated lesioning approach, where each node is in turn disconnected from the network. For each case, we evaluated how resultant changes to connectivity (quantified using a range of node-specific graph-theoretical metrics (Bullmore and Sporns, 2009)) relate to the functional dynamics (metastability and synchrony), both globally and in the neighbourhood of each node. In doing so, we tested the hypotheses that the structural importance of a node, systematically quantified using graph theoretical measures, should be related to the dynamical changes resulting from its removal and that the effects of lesions should be most important in the neighbourhood of each lesioned node.

Results indicate several relationships between structural properties of removed nodes and the effect of their removal on dynamics. Notably, one relationship provides an interesting mechanistic link between several recent empirical functional studies, related respectively to the network effects of focal strokes on modularity (Gratton et al., 2012) and cognition (Warren et al., 2014), and to dynamical lability in time-resolved functional connectomes (Zalesky et al., 2014).

Methods

Empirical connectivity and tract length data

We used 66 cortical ROI connectivity and tract length matrices, down-sampled from 998 cortical ROI data from Hagmann et al. (2008), which comprise a symmetric, weighted connectivity matrix derived from five healthy volunteers using diffusion spectrum imaging. The symmetric 66 ROI connectivity matrix was constructed by averaging two matrices, obtained by down-sampling the original 998 ROI connectivity matrix by incoming and outgoing connections respectively. For full details concerning the derivation of the 998 ROI matrix, see Hagmann et al. (2008).

Kuramoto model of coupled oscillators

We considered each node as an oscillator, and modelled their dynamical interactions using a variant of the Kuramoto model of coupled oscillators (Kuramoto, 1984; Acebron et al., 2005; Breakspear et al., 2010). This variant takes into account conduction delays arising from the spatial embedding of the network combined with a finite signal propagation velocity (Cabral et al., 2011, 2014a; Hellyer et al., 2014). The use of the Kuramoto model relies on the assumption that local neural activity is periodic and its state can thus be described by a single variable, the phase. A further assumption is that the coupling between local neural populations is weak, to the extent that amplitude effects can be neglected (Daffertshofer and van Wijk, 2011). The evolution of the phase θ_i of each oscillator i over time is described by a set of coupled first-order differential equations:

$$\frac{d\theta_i(t)}{dt} = \omega_i + k\sum_{j=1}^{N} C_{ij} \cdot \sin\left(\theta_j(t - D_{ij}) - \theta_i(t)\right) + \eta_i(t). \quad (1)$$

The rate of change of the phase $\theta_i(t)$ of each oscillator is given by its natural frequency ω_i and its interaction with the other oscillators, as well as an optional noise term $\eta_i(t)$. The intrinsic frequency was set to lie within the gamma frequency band, as gamma-band local field potential power has been shown to be coupled to BOLD fMRI signal and to be representative of overall local neuronal activity (Nir et al., 2007). To ensure robustness of the results with respect to frequency dispersion and noise, both naturally present in the brain (Faisal et al. 2008; Ghosh et al. 2008), we used two sets of conditions — "uniform", with all oscillators at 60 Hz and no added noise, and "noisy", with a normal distribution of frequencies with mean = 60 Hz, standard deviation = 3 Hz, combined with Gaussian white noise with mean = 0, standard deviation = 2 radians/s. (For a discussion of the minimal dependence of results on the chosen frequency of oscillations, please see the supplementary information.)

Interactions between oscillators are constrained by the relative coupling between them, given by the empirical connectivity matrix C_{ij}, and the propagation delays matrix D_{ij} (ms), determined using $D_{ij} = L_{ij} / v$, with L_{ij} (mm) the empirical tract length matrix and v (m/s) the mean conduction velocity. In turn, $v = \overline{L} / \tau$, or the mean tract length divided by the mean delay. The global behaviour of the model can be tuned using two parameters — the mean coupling k and the mean delay τ (ms).

The model was implemented in MATLAB (MathWorks), using a variant of the Euler method adapted to noise (Platen, 1999). We used an integration step-size of 0.1 ms, simulating phases at the millisecond resolution.

Dynamical metrics

In a system of oscillators such as the Kuramoto model, the global level of coherence can be evaluated using the order parameter, also called the mean field:

$$R(t)e^{i\phi(t)} = \frac{1}{N}\sum_{n=1}^{N} e^{i\theta_n(t)}. \quad (2)$$

The $e^{i\theta_n(t)}$ term describes the instantaneous position of oscillator n on the unit circle, whilst its mean over a set of oscillators captures their level of instantaneous synchronization. Specifically, the order parameter amplitude $R(t)$ quantifies the coherence of oscillators at time t — it can take values ranging from 0 for complete incoherence, to 1 for full coherence. We describe global dynamical behaviour of the model using the mean and the standard deviation of the order parameter amplitude

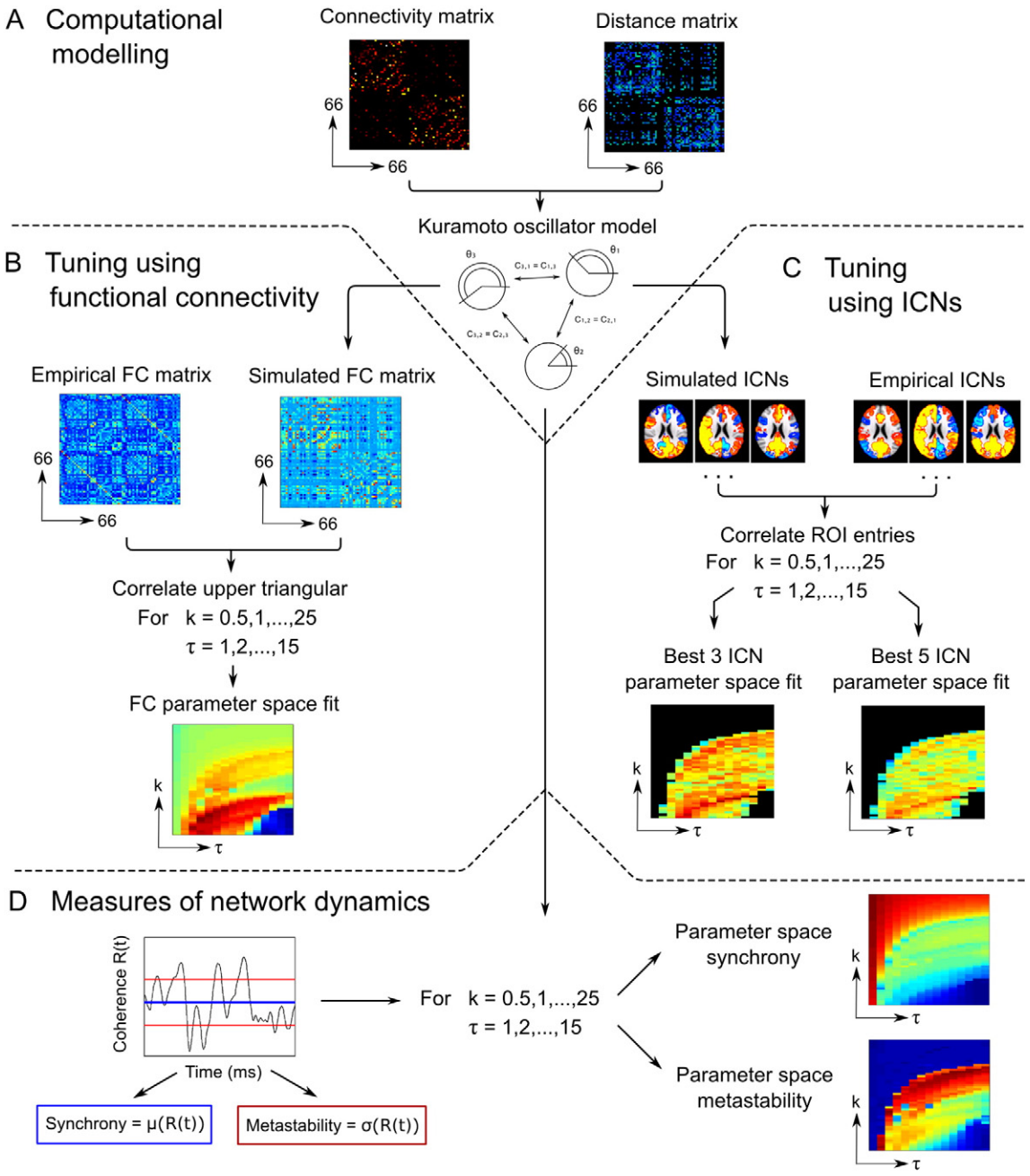

Fig. 1. Summary of model tuning methods. (A) Dynamics were simulated using the Kuramoto oscillator model, and simulated pairwise functional connectivity and intrinsic connectivity networks (ICNs) were extracted. The model was then tuned using (B) empirical pairwise functional connectivity and (C) empirical ICNs. Finally, (D) dynamical measures of global synchrony and metastability were calculated across parameter space.

over a time-course, which indicate respectively the global synchrony and the global metastability of the system (Fig. 1D) (Shanahan, 2010). Metastability is zero if the system is either completely synchronized or completely de-synchronized — a high value is present only when periods of coherence alternate with periods of incoherence (Shanahan, 2010).

The convergence of global synchrony and global metastability as a function of the duration of the simulated time-course and of the number of runs with different initial conditions taken into account is discussed in the supplementary information.

Empirical tuning methods (Fig. 1)

First, model behaviour was tuned with respect to empirical fMRI data to determine the mean coupling and delay scaling parameters for which the model behaves like the human brain. The range of parameter values studied was guided by previous findings of Cabral et al. (2011), with values of mean delay τ located in the physiologically realistic range ($1\ \text{ms} < \tau < 15\ \text{ms}$ at a resolution of 1 ms, $0.5 < k < 25$ at a resolution of 0.5). To preserve tight control over the behaviour of the model, we used the same initial conditions for each point when exploring the parameter space. For each position in parameter space, the simulation was run for 660 s. To eliminate dependence of results on initial transient periods, we discarded the initial 60 s of model output. Post-processing of phases, such as filtering or use of the Balloon–Windkessel model was avoided to prevent alteration of the results by such steps. It has been shown that the predictive power of a number of models, including the Kuramoto model, is largely insensitive to the presence of the hemodynamic model (Messé et al., 2014). Rather, we preserved

the model in its simple form, sufficient to capture dynamical interactions between nodes.

Tuning using functional connectivity (FC)

The first model tuning method compared time-averaged pair-wise FC within the model to empirical FC data from fMRI. Model FC was evaluated using pair-wise correlation (Pearson's r) between node activity time-courses, leading to a 66 × 66 region correlation matrix for each set of model parameters. We then compared this connectivity matrix with published empirical functional connectivity (measured in the same 5 subjects as the structural connectivity data) (Honey et al., 2009) using Pearson's correlations between their upper triangular parts (Fig. 1B).

Tuning using intrinsic connectivity networks

Whilst simple time-averaged measures of FC capture a broad overview of functional interactions within the brain, individual regions of the brain are involved in a range of different spatial interactions across time, known as intrinsic connectivity networks (ICNs); these can be examined using methods such as independent component analysis (ICA) (Beckmann et al., 2005). Here, we explored a second approach to model tuning by using ICA to extract simulated ICNs from model time-courses, and comparing these to a set of canonical empirical ICNs from Smith et al. (2009). Briefly, ICNs capture the major components of common functional interaction across subjects. For details regarding derivation of empirical ICNs, see (Smith et al., 2009). To allow direct comparability with modelled ICNs, we re-sampled empirical results into the space of 66 cortical ROIs of our model.

Modelled ICNs were extracted using standard methodology for extracting empirical ICNs from fMRI data — MELODIC from FSL (FMRIB, Beckmann et al., 2005). After formatting modelled data to match the standard MELODIC input format, we extracted 10 components, or ICNs, from model time-courses. For model parameters where synchronous dynamics were extreme (i.e., very asynchronous noisy dynamics, or full synchrony), the ICA algorithm failed to converge, either because there was no consistent correlation structure within the dataset over time, or because all regions of the model were fully correlated. Thus, we limited the ICN tuning method to parameter space coordinates where the dynamics exhibited sufficient variability for the MELODIC algorithm to converge (global metastability of 0.05 or above). To reduce computational complexity, we down-sampled time-courses at 0.2-second resolution, resulting in a collection of modelled ICN maps to compare against the empirical data using Pearson's correlations. Since the order of components extracted by MELODIC varies, we determined maximal correspondence between empirical and model components by calculating the pair-wise correlation between them and reordering the resulting correlation matrix so as to maximize entries along the diagonal. As the model is currently able to reproduce only a limited number of meaningful components, with the remaining ones consisting essentially of noise, we only took into account several of the best-matching components when calculating parameter space cost functions. To limit dependence of results on the number of components taken into account, we produced two main versions of the parameter space cost functions, taking into account the best-matching 3 and 5 components from modelled and empirical data respectively (Fig. 1C).

Lesion study (Fig. 2)

Following model tuning, we investigated the relationship between local structure and both global and neighbourhood dynamics. First, we characterized structural properties of each node in the intact network using the main local graph theoretical metrics. These include the main measures of connectivity centrality — the *degree* (number of edges connected to a node) and the *strength* (sum of the weights of edges

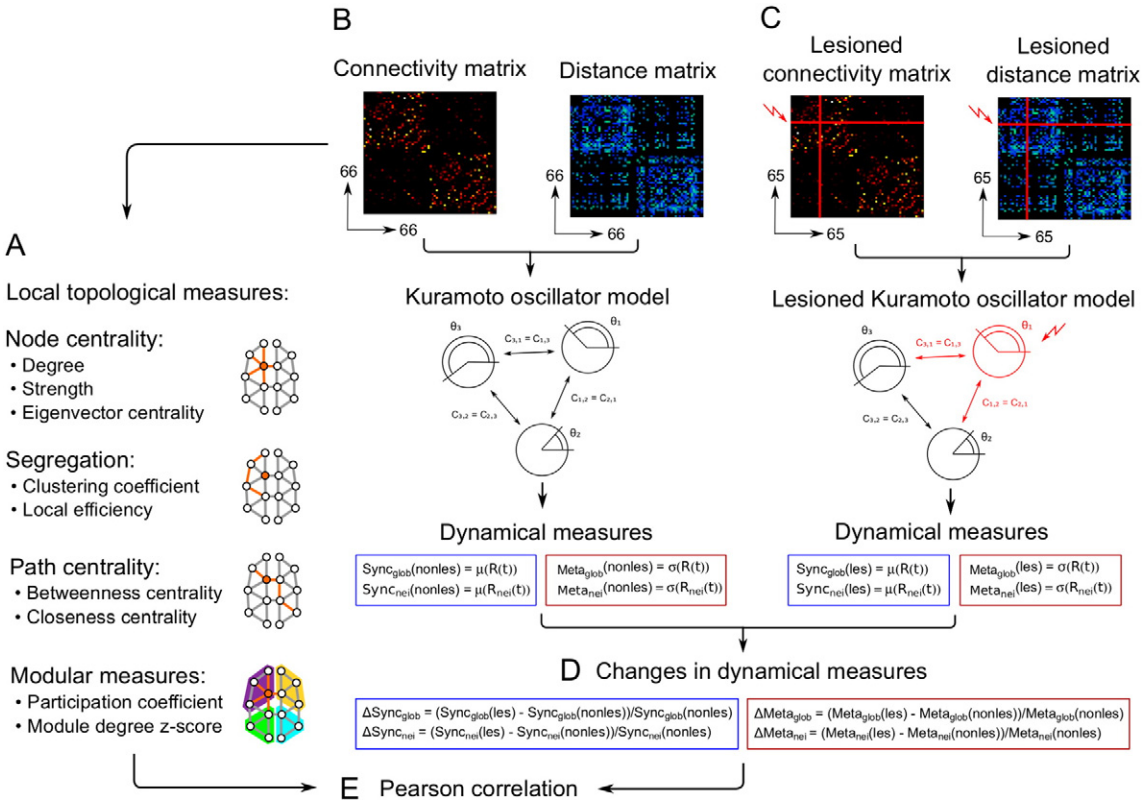

Fig. 2. Summary of lesion study methods. (A) Nine local topological measures were calculated for each node of the connectome. Dynamics were simulated on both (B) the intact connectome and (C) all instances of lesioned connectomes (with one node and all of its connections removed) and dynamical measures were calculated for both. (D) Changes in dynamical measures as a result of lesion were calculated, globally and in the neighbourhood of the lesioned node. (E) These were then correlated with the structural measures, to study the relationship between structural properties of the lesioned node and the effect of its removal on dynamics.

connected to a node). Moreover, we calculated each node's *eigenvector centrality*, a self-referential measure of centrality — nodes have high eigenvector centrality if they are connected to nodes which themselves have high eigenvector centrality (Newman, 2010). We then evaluated two local measures of segregation — the *clustering coefficient*, or fraction of all possible edges linking a node's neighbours, and the *local efficiency*, or the inverse average shortest path length between a node's neighbours. Furthermore, we evaluated two measures of path centrality — the *betweenness centrality*, quantifying the fraction of shortest paths within the network traversing a node, and the *closeness centrality*, which is the inverse topological distance between a node and all others. Finally, we evaluated two measures dependent on a prior definition of network modules — densely intra-connected but sparsely inter-connected components of the network. These measures are the *participation coefficient*, which quantifies the diversity of a node's inter-modular connections, and the *within-module degree z-score*, which measures how well-connected a node is to other nodes within its module. The module definition used was a six-module partition reported for this connectome dataset by Hagmann et al. (2008). Metrics were evaluated using the Brain Connectivity Toolbox (Rubinov and Sporns, 2010). For exact definitions of the structural metrics used, see supplementary information.

Next, we simulated dynamics in the intact connectome using 50 sets of random initial conditions, for 60 s, discarding the initial 10-second transients. In addition to assessing the synchrony and metastability globally, we evaluated these dynamical measures locally, amongst the neighbours of each node, to better characterize effects of node removal on network dynamics. Neighbourhood dynamical metrics were determined using the order parameter from Eq. (2), except evaluated over relevant subsets of nodes only, rather than the whole connectome.

We then removed, in turn, each node and all its connections, producing 66 lesioned connectomes with 65 nodes each. For each lesioned connectome, we simulated the resulting dynamics with conditions identical to the intact case. Again, we evaluated synchrony and metastability both globally and amongst the neighbours of the removed node.

To assess the effect of lesions on dynamics, we calculated changes in global and neighbourhood dynamics relative to global or neighbourhood dynamics in the unlesioned network. For each set of initial conditions, we calculated the difference in global and neighbourhood synchrony and metastability as a result of the lesion, normalised by the relevant dynamical measure (synchrony or metastability, global or neighbourhood) in the unlesioned network. We then averaged these percentage changes over initial conditions, to obtain a robust indication of changes in dynamics. Then, to assess whether structural properties of a node predict changes in dynamical metrics resulting from its removal, we calculated Pearson's correlation coefficients between structural nodal measures and changes in global and neighbourhood dynamics resulting from their removal. We corrected for multiple comparisons for each scale — global or neighbourhood, and for each set of simulation conditions — uniform or noisy. For each of those, we corrected the 18 comparisons (9 topological measures × 2 dynamical measures) using both the Bonferroni and the false discovery rate (FDR) corrections for multiple comparisons (Benjamini and Hochberg, 1995).

Results

All results reported below refer to uniform conditions, as noisy condition results are qualitatively the same. Results obtained with frequency dispersion and noise are located in the supplementary information.

Tuning using empirical fMRI data

Results from the FC tuning (Fig. 3A) indicate the range of parameters (couplings k and delays τ) of maximal correlation between modelled and empirical FC matrices. The rather low maximum values indicate that the model in its current form is unable to reproduce empirical data trends perfectly, which is unsurprising given the relative simplicity of the model and the coarseness of the input structural connectome. Still, a clear pattern exists, which is sufficient to identify an area of parameter space where the model best approximates empirical data. Results from the ICN tuning complement those from the FC results,

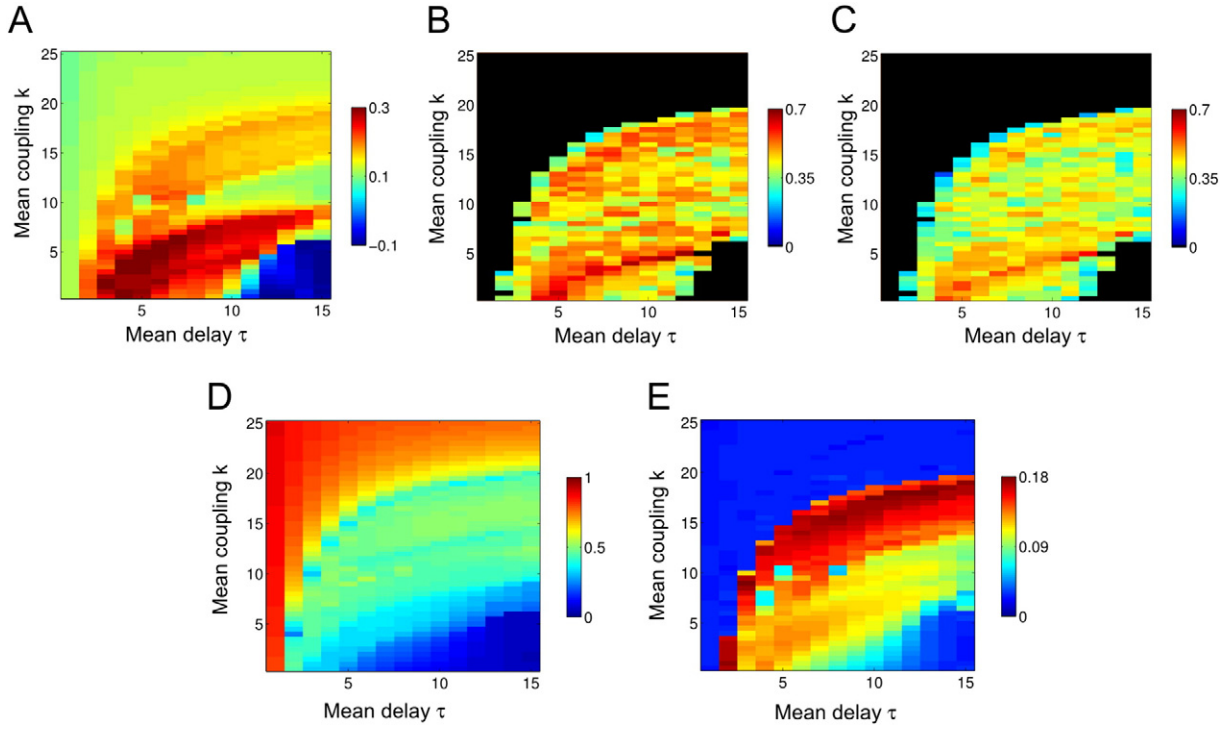

Fig. 3. Parameter space tuning cost functions and global model dynamics across parameter space. (A) Correlations of the upper triangular part of simulated and empirical FC matrices. Correlations of the (B) 3 best-matching simulated and empirical ICNs and (C) 5 best-matching simulated and empirical ICNs. (D) Global synchrony and (E) global metastability.

indicating the same range of parameters as providing the best match between modelled and empirical data (Figs. 3B + C). In this range of parameters the oscillators are only moderately synchronized ($0.2 < \overline{R} < 0.5$) and the amplitude of the order parameter fluctuates over time, which is indicative of a metastable regime (Figs. 3D + E).

A visualization of the best-matching empirical ICNs and their modelled counterparts is depicted in Fig. 4. The five best-matching ICNs (based on labels provided by Smith et al., 2009) were respectively the visual network, the default-mode network, the left-lateralized fronto-parietal network, the executive network and the auditory network.

The parameter space exploration allowed us to choose a set of parameters for further investigation of the structure–dynamics relationships. There is a range of parameters at which the crossover between empirical and modelled functional connectivity is optimal. To simplify further computation, we restrict the delay dimension to a biologically plausible 7 ms, which along with a mean tract length of 64.2 mm corresponds to a conduction velocity of 9.2 m/s — firmly in the range of physiologically realistic values for white matter tracts, estimated at 5–20 m/s (Waxman, 2006). Still, an issue linked with the use of several tuning methods is the fact that the cost functions associated to these can present variable maxima. Thus, we chose a set of parameters which does not correspond to a strict maximum on either of the three cost functions, but still presents high correlations on all three. We chose $k = 3.5$, $\tau = 7$, where the values of Pearson's correlation were $r = 0.27$, $p < 10^{-10}$ for the FC tuning, $r = 0.63$, $p < 10^{-10}$ for the best-matching 3 ICNs and $r = 0.54$, $p < 10^{-10}$ for the best-matching 5 ICNs, with synchrony = 0.31 and metastability = 0.12. Plots of correlations between empirical and modelled FC and ICNs at the chosen point in parameter space are located in supplementary figure S3. Details of the maxima of correlations between simulated and empirical data, for all three tuning approaches used, are reported in the supplementary information.

To ascertain the non-random nature of simulated dynamics, we have generated a null model. A set of 100 randomized connectivity matrices was used to simulate dynamics, which were quantified using dynamical measures of synchrony and metastability, and compared to empirical data using the FC and ICN methods. Both dynamical measures and correlations with empirical data were significantly higher when simulating dynamics using non-random connectivity, compared to the randomly generated null distributions ($p < 10^{-10}$ in all cases). For details, see supplementary information.

Effect of lesions on global dynamics

In order to understand the relationship between connectome structure and dynamics, we investigated the effect of lesioning individual nodes, first on global dynamics and then on local dynamics (section *Effects of lesions on neighbourhood dynamics*). Most nodes when lesioned lead to small, but significant decreases in global synchrony (average change −1.7%, 95% confidence interval (CI) [−3.0%, −0.4%], two-tailed *t*-test, $p = 0.017$), with a slight spatial bias, whereby decreases in global synchrony generally seem to be caused by lesions to nodes within the parietal and occipital cortex (Fig. 5A). Changes in global metastability seem more balanced, in that both increases and decreases occur (Fig. 5B). Moreover, the larger changes cannot be attributed to several "outlier" nodes. Increases in global metastability are predominantly seen in lesions of nodes closer to the midline, whilst lesions of lateral nodes are associated with decreases in global metastability. On average, lesions lead to decreases in global metastability (average change −0.9%, 95% CI [−1.8%, −0.05%], two-tailed *t*-test, $p = 0.035$). Finally, we note that there is no relationship between changes in the two global metrics (synchrony and metastability) following node lesioning (Pearson's $r = -0.01$, $p = 0.92$).

In order to understand why lesions of different nodes had different effects on global dynamics, changes in global synchrony and metastability were related to a range of graph theoretical metrics. Full results of relative changes in global and neighbourhood synchrony and metastability as a function of the nine local structural metrics are listed in Table 1. In addition, those correlations which survived Bonferroni and/or FDR correction are visualized in Fig. 6. The eigenvector centrality of a node is significantly negatively correlated to changes in both global synchrony ($r = -0.38$, $p = 0.0019$) and positively correlated to changes in global metastability ($r = 0.41$, $p = 0.00076$) following its lesioning. Increases in global metastability are also strongly associated with lesions to nodes with high participation coefficient ($r = 0.46$, $p = 0.00010$).

Effects of lesions on neighbourhood dynamics

In order to better characterize dynamical changes following lesions, we estimated changes in network dynamics amongst the group of nodes that are directly connected to the lesioned node. As in the case of global synchrony, changes in neighbourhood synchrony are significantly negative overall (average change −5.1%, 95% CI [−7.1%, −3.1%], two-tailed *t*-test, $p = 3.5e-6$). Moreover, changes in neighbourhood metastability are, on average, not significantly different from 0 (average change +1.7%, 95% CI [−1.0%, +4.4%], two-tailed *t*-test, $p = 0.21$).

Lesioned node strength is predictive of changes in both neighbourhood synchrony ($r = -0.33$, $p = 0.0080$) and metastability ($r = 0.38$, $p = 0.0022$). Again, lesioned node eigenvector centrality predicts changes in both neighbourhood synchrony ($r = -0.42$, $p = 0.00055$) and metastability ($r = 0.67$, $p = 1.6e-9$). Moreover, local clustering is predictive of changes in neighbourhood metastability — as indicated by both the local efficiency of the lesioned node ($r = 0.35$, $p = 0.0044$) and its clustering coefficient ($r = 0.42$, $p = 0.00050$). Finally, changes in neighbourhood metastability are also predicted by the participation coefficient of the lesioned node ($r = 0.42$, $p = 0.00060$). As in the case of

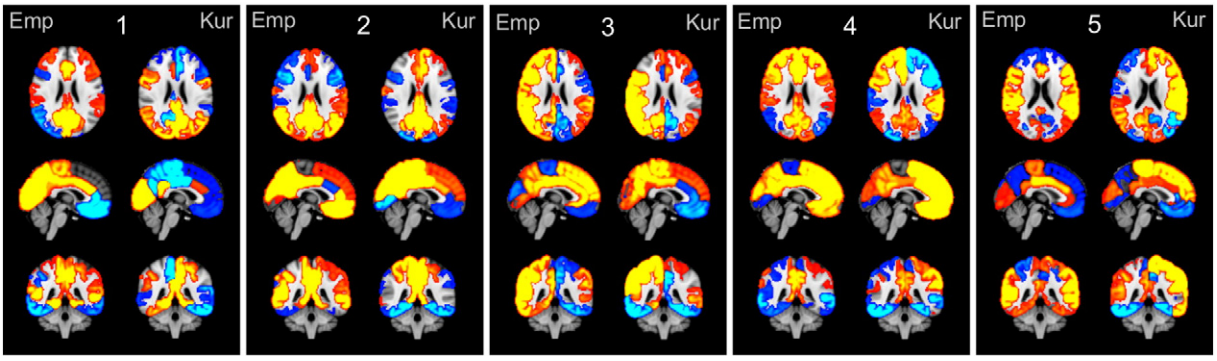

Fig. 4. Visualization of the five best-matching empirical ICNs and their simulated counterparts. The five best-matching ICNs (based on labels provided by Smith et al., 2009) were respectively the visual network, the default-mode network, the left-lateralized fronto-parietal network, the executive network and the auditory network. ICNs are depicted as Z-score maps, where warm colors correspond to positive Z-scores and cold colors to negative Z-scores.

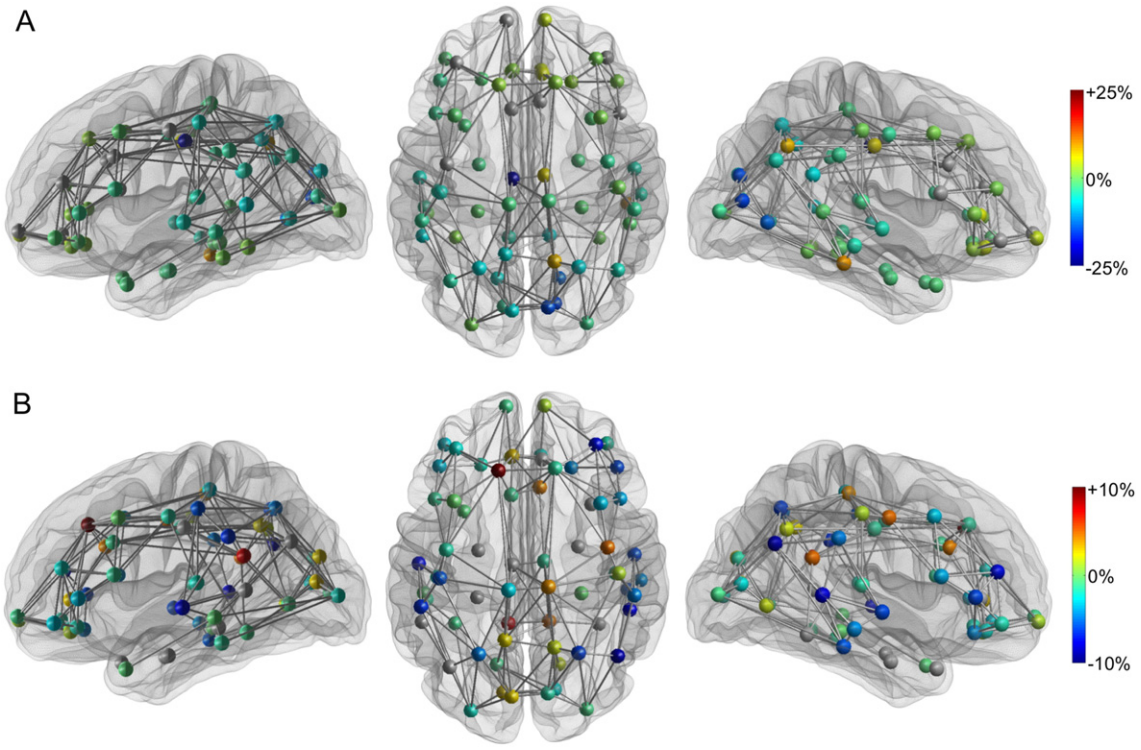

Fig. 5. Visualization of the effects of node lesions on (A) global synchrony and (B) global metastability. Only nodes for which the change in dynamical measures was significantly different from 0 (two-tailed paired *t*-test across the 50 sets of initial conditions used) are coloured; the rest are grey. Warmer colours correspond to increases in dynamical measures, colder colours correspond to decreases. For clarity, only the 30% strongest edges are depicted.

global dynamics, cases where a structural metric predicts changes in both synchrony and metastability exhibit opposite signs. Correlations of structural metrics with changes in synchrony are negative, in that lesions of topologically more important nodes lead to greater decreases in neighbourhood synchrony, whereas correlations of structural measures are positively associated with changes in metastability, indicating that lesions of topologically more important nodes lead to smaller decreases, or greater increases, in neighbourhood metastability.

Discussion

Using an empirically calibrated computational model of macroscopic neural dynamics, we investigated the relationship between structural properties of individual network nodes and brain dynamics. This new approach reveals relationships between local network structure and global and local network synchrony and metastability, corroborating our hypothesis that the structural importance of connectome nodes, systematically quantified using a range of node-specific graph-theoretical measures, is related to the changes in dynamics following the removal of these nodes. As we consider below, our findings provide a mechanistic framework to understand recent neuroimaging findings relating to network effects of focal strokes (Gratton et al., 2012; Warren et al. 2014) and dynamical lability in time-resolved functional connectomes (Zalesky et al., 2014).

Relation of model to empirical data

Both the pairwise FC and ICN tuning methods provided similar results, identifying overlapping regions of parameter space where simulated data exhibit highest correlations with empirical data. This is not surprising — even though the empirical FC matrices and ICN networks used for tuning originate from distinct fMRI datasets, both consist of resting-state data, known to exhibit highly consistent features across cohorts of healthy subjects (Biswal et al., 2010; Pendse et al., 2011; Chou et al. 2012). Moreover, the methods used for data processing — pairwise correlations to obtain FC matrices and ICA to obtain ICNs, extract related features of functional interaction from the data. The FC matrix method is simpler to use. However, the advantage of the ICN tuning method is that it extracts the main components of co-activation from the simulated data. It thus places greater importance on major modes of dynamical interaction, disregarding the erroneous interactions inherently present in the simulated data, which decrease the similarity of the simulated time-courses with empirical data. This might be the reason why the ICN tuning method identifies a narrower portion of parameter space as exhibiting highest correlations with empirical data.

Rather than a distinct coordinate, both tuning methods identify a portion of parameter space where simulated data exhibit high correlations with empirical fMRI data. Whilst the tuning methods used present distinct maxima (reported in supplementary information), we suspect that the behaviour of the model would be similar at all points on the "ridge" of high correlation with empirical data. Although the coupling parameter k lacks a clear physiological counterpart, the choice of a delay parameter τ that corresponds to a realistic axonal conduction velocity narrows down parameter choice due to the shape of the high-correlation "ridge".

The idea that computational models of brain dynamics exhibit correlation patterns comparable to ICNs is not novel. It is implicit in the study of Cabral et al. (2011), who have studied network connectivity in a seed-based manner. Moreover, Haimovici et al. (2013) have shown that within a computational model of brain dynamics, patterns most strongly resembling empirical ICNs appear when the system is at criticality, a dynamical regime situated between order and disorder, which exhibits both correlations between activity of distant areas and sufficient variability for communication to occur (Kitzbichler et al., 2009; Beggs and Timme, 2012). Interestingly, the ICN-like patterns were lost for sub- or super-critical dynamics, indicating that criticality might be an important property of healthy brain dynamics (Haimovici et al., 2013). Our findings align with these results, in that our chosen

Table 1
All correlations between structural properties of individual nodes and the effect of their lesion on global and neighbourhood dynamics. Correlations which survive either multiple comparison correction method are highlighted in bold and marked with (b) if surviving the more conservative Bonferroni correction, or (f) if surviving the false discovery rate (FDR). p-Values are included for correlations with $p \leq 0.1$; the remaining correlations are marked as not significant (NS).

		Degree	Strength	Eigenvector centrality	Clustering coefficient	Local efficiency	Closeness centrality	Betweenness centrality	Participation coefficient	Degree z-score
Global	Δ Synchrony	−0.06 (NS)	−0.27 (0.027)	**−0.38 (0.0019) b**	−0.20 (NS)	−0.22 (0.074)	−0.23 (0.071)	−0.15 (NS)	−0.11 (NS)	−0.18 (NS)
	Δ Metastability	0.13 (NS)	0.19 (NS)	**0.41(0.00076) b**	0.03 (NS)	0.11 (NS)	0.19 (NS)	0.26 (0.040)	**0.46 (0.00010) b**	−0.18 (NS)
Neighbourhood	Δ Synchrony	−0.13 (NS)	**−0.33 (0.0080) f**	**−0.42 (0.00055) b**	−0.15 (NS)	−0.20 (NS)	−0.25 (0.049)	−0.11 (NS)	0.01 (NS)	−0.22 (0.076)
	Δ Metastability	0.15 (NS)	**0.38 (0.0022) b**	**0.67 (1.6e−9) b**	0.26 (0.042)	**0.35 (0.0044) f**	**0.42 (0.00050) b**	0.24 (0.054)	**0.42 (0.00060) b**	0.00 (NS)

working point exhibits both high synchrony and metastability, indicative of criticality (Tognoli and Kelso, 2014), as well as correlation patterns resembling empirical ICNs. Additionally, two further recent studies demonstrated the emergence of ICNs similar to those found in resting-state fMRI in computational models of neural dynamics (Hansen et al., 2015; Ponce-Alvarez et al., 2015).

Relationship between local structure and global dynamics

Within the spatial distribution of changes in global synchrony and metastability, visualized in Fig. 5, we note that decreases in global synchrony generally seem to be caused by lesions to posterior regions. This is in agreement with the role of these regions as the highly connected structural core of the cerebral cortex (Hagmann et al., 2008) and, in turn, with findings demonstrating that synchrony between node pairs increases with the number of neighbours they share (Vuksanovic and Hövel, 2014). In contrast, decreases in metastability seem to be caused by lesions of lateral nodes, whilst its increases seem to be caused by lesions along the midline. Thus, lateral regions appear to keep baseline metastability high, whereas midline regions can be seen as inhibiting it.

Using graph theory to quantify structural properties of lesioned nodes, we found three significant relationships between local structure and global dynamics.

Lesions of nodes with higher eigenvector centrality lead to significantly greater decreases in global synchrony, and significantly greater increases in global metastability. Nodes have high eigenvector centrality if they are connected to nodes which themselves are highly central (Newman, 2010). A node situated on the periphery, which would exhibit low degree or betweenness centrality, could possess high eigenvector centrality by sharing a connection with a highly central node. The finding that the role of individual nodes in controlling stability and flexibility of global neural dynamics is largely determined by the centrality of their neighbours extends the role of the eigenvector centrality measure, shown to be useful in analyzing connectivity patterns in fMRI data (Lohmann et al., 2010) as well as a potential biomarker of Alzheimer's disease progression (Binnewijzend et al., 2014).

A further correlation is present at the global dynamics level, between the participation coefficient of a node, which quantifies the diversity of its inter-modular connections (Guimera and Amaral, 2005), and the change in metastability following its lesioning. The participation coefficient of nodes with connections distributed fairly uniformly across all network modules would tend to one, whilst for nodes with all connections within one module it would be zero. Thus, nodes with a high participation coefficient are integrative or connector hubs, known to play an important role in integrating otherwise segregated processes (Sporns et al. 2007; Honey and Sporns, 2008; Shanahan, 2012). The disruptive effects of lesioning hub regions on dynamics and function have been demonstrated previously (Honey and Sporns., 2008; Alstott et al. 2009). Moreover, numerous integrative hubs of the connectome lie near the midline (Hagmann et al., 2008), as reflected in the spatial trend observed in global metastability changes (Fig. 5), where lesions to midline nodes generally lead to increases in global metastability. Since modules are by definition strongly intra-connected and weakly inter-connected, they facilitate localized synchrony. Thus, the significant relationship of neural dynamics with a modularity-dependent metric aligns with findings of Cabral et al. (2011), who reported globally incoherent clusters of locally synchronous activity in a Kuramoto model with similarly low values of mean coupling and delay.

Nodes with high eigenvector centrality and participation coefficient are likely members of the rich club (van den Heuvel and Sporns, 2011), a set of densely mutually interconnected hub nodes that forms a backbone for shortest communication paths in the connectome (van den Heuvel et al., 2012). The densely connected core of rich club regions has been shown to serve as an anatomical substrate for the "transmodal" integration of functional networks involving low-degree

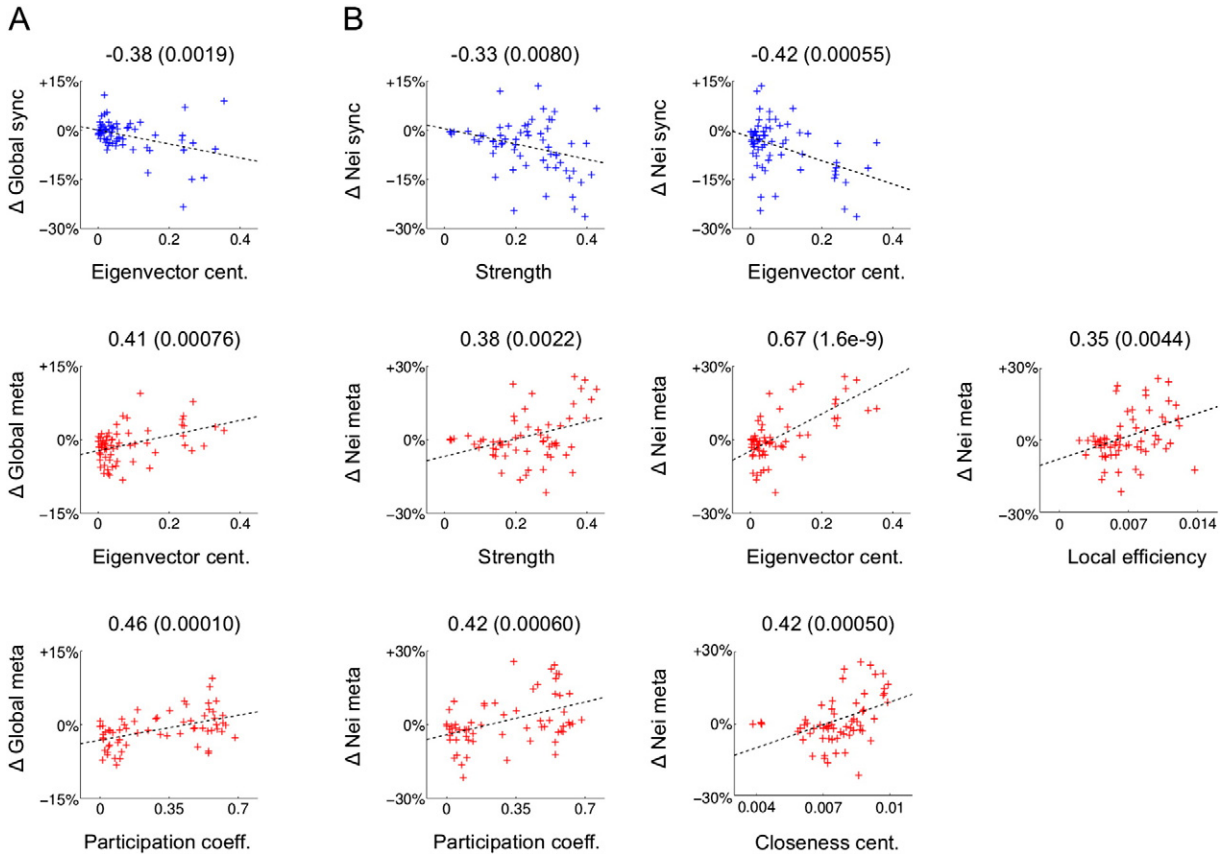

Fig. 6. Correlations between structural measures and changes in dynamics which survive multiple comparisons correction. Results of Pearson's correlations are situated above each plot, as $r(p)$. (A) Correlations of structural measures with changes in global dynamical measures. (B) Correlations of structural measures with neighbourhood dynamical measures.

peripheral regions, both in empirical (Leech et al. 2012; Braga et al., 2013; van den Heuvel and Sporns, 2013) and computational studies (Senden et al., 2014), in line with the possible role of the rich club as a global neuronal workspace (Baars, 2005; Senden et al., 2014). Recently, the rich club has been shown to promote slow and stable dynamical activity, with surrounding peripheral nodes exhibiting faster and less stable dynamics (Gollo et al., 2015). Our results, demonstrating that lesions to core (/peripheral) nodes with high (/low) participation and centrality lead to increases (/decreases) in metastability, are in line with these findings. The Kuramoto model would be suitable for further studies of the role of the rich club in cortical dynamics, as its order parameter can be conveniently evaluated over subsets of nodes corresponding to different levels of the rich club.

Relationship between local structure and local dynamics

When considering neighbourhood dynamics, we found numerous significant correlations between graph theoretical topological properties of individual nodes and the local dynamical changes following their lesioning. Neighbourhood findings related to the eigenvector centrality and participation coefficient parallel the global case. In addition, changes in both neighbourhood synchrony and metastability were predicted by the strength of the lesioned node, whilst changes in neighbourhood metastability were also predicted by the local efficiency and closeness centrality of the removed node.

Interestingly, nodal strength and eigenvector centrality are predictive of changes in local dynamics following lesions, but the nodal degree is not. The number of connections a node shares with its neighbours was postulated as the simplest measure of nodal importance as well as the most interpretable graph theoretical measure (Rubinov and Sporns, 2010). In a previous simulation study, Honey and Sporns (2008) found that perturbations of high-degree nodes produced the most widespread effects on dynamics, although this disparity might be caused by the binary connectomes they used as well as the fully synchronized regime of their Kuramoto model. Moreover, Tewarie et al. (2014) found that degrees of structurally connected regions are important predictors of functional connectivity between them, although the binary connectomes they used again prevented them from investigating the effect of node strength. However, in the context of metastable neural dynamics, the relative importance of individual connections clearly provides valuable information. Indeed, Cabral et al. (2014a) have demonstrated that the current model of coupled Kuramoto oscillators exhibits neither correspondence to empirical data, nor metastable dynamics in the extreme cases where connections are made homogeneous (all equally strong) or randomized (the specific modular connectivity structure of the human connectome is destroyed). Here, we have confirmed the importance of the connectome's structure in generating metastable dynamics which match empirical results, using a conservative null model where connections are randomized whilst preserving the degree distribution and ensuring realistic delays (for details, see the supplementary information).

As hypothesized, a greater number of relationships between graph-theoretical structural properties of nodes and dynamics was present when evaluating changes in dynamics in the neighbourhood of lesioned nodes than when quantifying changes in global dynamics. This may be related to a loss of detail when evaluating the order parameter over all nodes rather than to a lack of changes in dynamics at locations distant to the lesion. Diaschisis is a known phenomenon whereby neurophysiological changes occur at sites distal to the brain lesion (Carera and Tononi, 2014). It would be interesting, in a future study, to systematically

investigate changes in local dynamics within subsets of nodes distal to the lesioned ones. One potential approach would be to restrict model tuning to the pairwise FC method, reserving ICNs as a set of hypothetically affected networks distal from the lesion site.

Integrative hubs, modularity and cortical dynamics

Computational lesion studies are a popular theoretical tool to understand brain network connectivity. For example, they have been used to study the structural robustness of cortical networks (Hagmann et al., 2007; Kaiser et al., 2007), to identify the core white matter scaffold of the human brain (Irimia and Van Horn, 2014) or to demonstrate a link between the brain's resilience to systematic insults and IQ, suggesting intelligence as a predictor of post-lesional recovery (Santarnecchi et al., 2015). Computational lesion studies can also be compared to neurological studies of altered structure and cortical dynamics in patients with lesions following focal stroke.

Gratton et al. (2012) studied connectomes of 35 patients with focal strokes, and reported a negative relationship between the participation coefficient of damaged areas and the modularity of the resulting functional dynamics. Thus, their study confirms the importance of connector hubs for functional network dynamics. Moreover, the reported effects spread into the unlesioned hemisphere. The observation of both local and global relationships between focal lesions and alterations in neural function is consistent with the findings of our simulations, which offer a mechanistic explanation of how such structural damage can result in altered neural dynamics.

A recent study by Zalesky et al. (2014) provides further empirical support to the relationships observed in our simulated lesion study. Zalesky et al. used the novel framework of time-resolved functional connectomics to study the dynamics of intra- and inter-modular connections. Intra-modular connections tended to be more stable over time, whilst inter-modular connections were dynamically more labile, alternating between positive and negative correlations. These findings are in contrast to standard time-averaged functional connectivity studies (e.g., Gratton et al., 2012), where the activity of inter-modular connections is averaged over time to low connectivity values, leading the algorithms used for modular partitioning to define the module boundaries precisely along those weak-appearing connections. The time-resolved study of Zalesky et al. (2014) shows that the inter-modular connections are not weaker, but rather more labile. Thus, an underlying cause of studies demonstrating decreases in the modularity of brain function might in reality be an increase of lability, or metastability, of the network dynamics. By demonstrating that metastability is significantly controlled by integrative hubs, our results provide a mechanistic link between the empirical studies of Gratton et al. (2012) and Zalesky et al. (2014). Together, these three studies form a triad, linking integrative hubs, variability of dynamics and modularity.

An additional recent empirical study, by Warren et al. (2014), supports the importance of the participation coefficient in local neuronal dynamics and, most interestingly, in cognition. Warren et al. studied 30 patients with focal lesions, 19 of which were to “target” regions with high participation coefficients, with the remaining ones to “control” regions with high degree only. Results of the study demonstrated more widespread deficits in cognition in patients with “target” lesions to high-participation nodes, whereas lesions to “control” nodes with only high degree in the remaining patients led to more circumscribed effects. As Warren et al. suggest, lesions to nodes with high participation coefficients disrupt communication between disparate cognitive networks, causing more damage than lesions of similar magnitude within a single functional network (Warren et al., 2014). However, in view of the present findings and their aforementioned link to studies by Gratton et al. (2012) and Zalesky et al. (2014), the cognitive deficits could further be interpreted as stemming from an increase in dynamical lability following lesions to nodes which in the undamaged network maintain healthy levels of synchrony and metastability.

Limitations

Simple, relatively abstract models such as the Kuramoto model are inherently limited in their ability to simulate functional connectivity data. One limitation of the Kuramoto model is the use of a sine function to describe the oscillator coupling. In general, the coupling function can be any 2π-periodic function of the difference in phases between oscillators (Pikovsky et al., 2001), and periodic functions containing more harmonics than the sine function studied by Kuramoto have been proposed (Acebron et al., 2005). However, the basic sine-function form of the Kuramoto model, adapted to incorporate realistic connectivity and time-delays, has been used to simulate whole-brain neural dynamics at low computational cost (Honey and Sporns, 2008; Breakspear et al., 2010; Shanahan, 2010; Cabral et al., 2011, 2014a; Hellyer et al., 2014). Moreover, features of Kuramoto model dynamics have been replicated using a more biologically realistic model of populations of coupled Hodgkin and Huxley neurons (Bhowmik and Shanahan, 2012), reinforcing its role as a candidate model to investigate spontaneous brain activity from a network perspective. Additionally, the Kuramoto model has been shown to hold similar predictive power to alternative computational models of whole-brain dynamics (Cabral et al., 2014b; Messé et al., 2014).

Still, the correspondence of the computational model with empirical data could be improved in several ways. As imaging and data processing methods improve, so will the quality of the obtained connectomes. In particular, the ability of DWI methods to capture long, inter-hemispheric tracts is currently limited, as noted by Hagmann et al. (2008). Such connections are associated with substantial predictive power, as their artificial addition to structural connectomes considerably increases the predictive power of generative models of neural dynamics (Deco et al., 2014; Messé et al., 2014). Additionally, a simple way to increase realism of the model would be to use a structural connectome that includes sub-cortical nodes, which are known to relay to many cortical nodes and are thus likely to play an important role in regulating neural dynamics.

The addition of subcortical nodes would also increase the relevance of such computational models to simulate the effects of stroke, which is known to often occur in subcortical regions (Corbetta et al. 2015). An additional way of simulating stroke effects more realistically would be to derive the distribution of lesions to the network from empirically-defined patterns observed in neurological studies. For example, cortical strokes often occur along the middle cerebral artery with characteristic distributions (Corbetta et al. 2015), and are likely to affect multiple nodes of the connectome. In the current work we studied individual nodes in isolation. An interesting avenue of future research would be to examine the effect on neural dynamics of lesions to groups of nodes, whose identities could be determined by clinical data. Moreover, damaged brain areas may still be active, but present altered activity. Computational modeling has been used to show that such alterations in activity lead to global decreases in functional connectivity, and that the impact of such alterations depends on the structural properties of their location within the cortical network (van Dellen et al. 2013).

Within the ICN tuning method, the chosen, highest-correlating components are not necessarily the same across parameter space. It would be interesting, in future work, to investigate the dependence of the “optimal” components on model parameters. Here, we tried to limit dependence on the number of components used by producing two parameter space maps, taking into account the best-matching 3 and 5 ICNs respectively.

In addition, we have not explored the dependence of the ICN tuning on ICA dimensionality, which is the number of components extracted from empirical or simulated data. We have focused on a low-dimensional decomposition, which is more widely used in the literature. We expect that a high-dimensional decomposition, which would result in smaller, more fractionated components, might not reproduce the overall patterns seen in empirical data as well.

A final limitation of the present work concerns the structural and dynamical metrics used. The graph-theoretical structural metrics only take into account the connectivity topology, whilst simulations of the dynamics implicate both the connectivity and the distances, which interact in a non-linear manner. Indeed, the spatial embedding of connectome nodes has been shown to be highly relevant (Deco et al., 2009; Bullmore and Sporns, 2012; Cabral et al., 2014a; Samu et al., 2014). Thus, devising ways of taking tract lengths into account explicitly when evaluating structural metrics might yield additional insights into structure–dynamics relationship within the connectome.

Future directions

In addition to the above specific suggestions for future work, a general avenue for further investigations concerns the relevance of mechanistic links between neural structure, function and dynamics to cognition, in health and disease. Hellyer et al. (2014) recently demonstrated the relevance of the metastability metric to cognition by using neuroimaging data and a Kuramoto model to study differences in neural dynamics between rest and a simple sustained attention task. Empirical and simulated results were in agreement, demonstrating a simultaneous increase in synchrony and reduction in metastability during a task state, consistent with a more constrained cognitive state relative to rest.

A range of studies on both time-resolved and static modularity suggest that modelling work similar to Hellyer et al. (2014) could be applied to relate the proposed mechanistic triad, linking modularity, integrative hubs and dynamical variability, to cognition, in health and disease. Indeed, modularity in time-resolved functional networks has been associated with learning (Bassett et al., 2011), providing support for hypotheses of relationships between functional connectome modularity and adaptability (Meunier et al., 2010). The clinical relevance of dynamical dwell-time in different modular states was demonstrated in a study on Alzheimer's patients (Jones et al., 2012). In addition, several studies have reported the relevance of time-averaged functional network modularity to cognition (Crossley et al., 2013), and particularly to memory (van Dellen et al., 2012; You et al., 2013; Gamboa et al., 2014; Meunier et al., 2014).

In general, the use of mechanistic models simulating macroscopic brain function and dynamics remains of paramount importance. Regardless of the specific model used, dynamical flexibility remains a highly relevant phenomenon that requires further attention. Related mechanisms, such as lability, have been previously discussed (Friston, 2001; Kitzbichler et al., 2009), and their relation to the present definition of metastability should be further explored. Moreover, such dynamical phenomena can be studied and characterized using other mathematical tools (Kelso, 2012; Tognoli and Kelso, 2014). For instance, phase-slips have been postulated as a hallmark feature of weakly coupled oscillators (Zheng et al., 1998, 2000) but their occurrence in simulations of neural dynamics based on empirical structural connectivity data has not yet been investigated. Furthermore, the occurrence of metastable chimera states, where synchrony nd de-synchrony simultaneously co-exist, has been shown in networks of artificially coupled oscillators (Shanahan, 2010; Wildie and Shanahan, 2012), and recently in human connectome data (Villegas et al., 2014). Going forward, further work exploring the stability of neural dynamics as well as simulations of mechanistic relationships between structure, function and dynamics could shed light on healthy cognitive processes and their breakdown in disease.

Acknowledgments

We would like to thank Patric Hagmann for providing the structural and functional connectomes used in this study. We would also like to thank two anonymous reviewers for their helpful and constructive feedback. FV was supported, during manuscript revision, by a Gates Cambridge Trust award. PJH was supported by a Medical Research Council doctoral training award. GS was supported by a clinical research fellowship awarded in the Wellcome Trust-GlaxoSmithKline Translational Medicine Training Programme. JC was supported by ERC Grant CAREGIVING (n. 615539).

Appendix A. Supplementary information

Supplementary information to this article can be found online at http://dx.doi.org/10.1016/j.neuroimage.2015.05.042.

References

Acebron, J.A., Bonilla, L.L., Perez Vicente, C.J., Ritort, F., Spigler, R., 2005. The Kuramoto model: a simple paradigm for synchronization phenomena. Rev. Mod. Phys. 77, 137–185.
Alstott, J., Breakspear, M., Hagmann, P., Cammoun, L., Sporns, O., 2009. Modeling the impact of lesions in the human brain. PLoS Comput. Biol. 5, e1000408.
Ashwin, P., Orosz, G., Wordsworth, J., Townley, S., 2007. Dynamics on networks of cluster states for globally coupled phase oscillators. SIAM J. Appl. Dyn. Syst. 6 (4), 728–758.
Baars, B.J., 2005. Global Workspace Theory of Consciousness: Toward a Cognitive Neuroscience of Human Experience. The Boundaries of Consciousness: Neurobiology and Neuropathology. 150 pp. 45–53.
Bassett, D.S., Wymbs, N.F., Porter, M.A., Mucha, P.J., Carlson, J.M., Grafton, S.T., 2011. Dynamic reconfiguration of human brain networks during learning. PNAS http://dx.doi.org/10.1073/pnas.1018985108.
Beckmann, C.F., DeLuca, M., Devlin, J.T., Smith, S.M., 2005. Investigations into resting-state connectivity using independent component analysis. Philos. Trans. R. Soc. B 360, 1001–1013.
Beggs, J.M., Timme, N., 2012. Being critical of criticality in the brain. Front. Physiol. 3, 163.
Benjamini, Y., Hochberg, Y., 1995. Controlling the false discovery rate: a practical and powerful approach to multiple testing. J. R. Stat. Soc. Ser. B 57, 289–300.
Bhowmik, D., Shanahan, M., 2012. How well do oscillator models capture the behaviour of biological neurons? Neural Networks (IJCNN), The 2012 International Joint Conference on pp. 1–8 10-15 June 2012. http://dx.doi.org/10.1109/IJCNN.2012.6252395
Binnewijzend, M.A.A., Adriaanse, S.M., Van der Flier, W.M., Teunissen, C.E., de Munck, J.C., Stam, C.J., Scheltens, P., van Berckel, B.N.M., Barkhof, F., Meije, Wink A., 2014. Brain network alterations in Alzheimer's disease measured by eigenvector centrality in fMRI are related to cognition and CSF biomarkers. Hum. Brain Mapp. 35, 2383–2393.
Biswal, B.B., Mennes, M., Zuo, X.N., Gohel, S., Kelly, C., Smith, S.M., Beckmann, C.F., Adelstein, J.S., Buckner, R.L., Colcombe, S., et al., 2010. Toward discovery science of human brain function. PNAS USA 107, 4734–4739.
Braga, R., Sharp, D.J., Leeson, C., Wise, R.J.S., Leech, R., 2013. Echoes of the brain within default mode, association and hetermodal cortices. J. Neurosci. 33 (35), 14031–14039.
Breakspear, M., Heitmann, S., Daffertshoffer, A., 2010. Generative models of cortical oscillations: neurobiological implications of the Kuramoto model. Front. Hum. Neurosci. http://dx.doi.org/10.3389/fnhum.2010.00190.
Buckner, R.L., Vincent, J.L., 2007. Unrest at rest: default activity and spontaneous network correlations. NeuroImage 37, 1091–1096.
Bullmore, E., Sporns, O., 2009. Complex brain networks: graph theoretical analysis of structural and functional systems. Nat. Rev. Neurosci. 10, 186–198.
Bullmore, E., Sporns, O., 2012. The economy of brain network organization. Nat. Rev. Neurosci. 13, 336–349.
Cabral, J., Hugues, E., Sporns, O., Deco, G., 2011. Role of local network oscillations in resting-state functional connectivity. NeuroImage 57, 130–139.
Cabral, J., Hugues, E., Kringelbach, M.L., Deco, G., 2012. Modelling the outcome of structural disconnection on resting-state functional connectivity. NeuroImage 62, 1342–1353.
Cabral, J., Luckhoo, H., Woolrich, M., Joensson, M., Mohseni, H., Baker, A., Kringelbach, M.L., Deco, G., 2014a. Exploring mechanisms of spontaneous functional connectivity in MEG: how delayed network interactions lead to structured amplitude envelopes of band-pass filtered oscillations. NeuroImage 90, 423–435.
Cabral, J., Kringelbach, M.L., Deco, G., 2014b. Exploring the network dynamics underlying brain activity during rest. Prog. Neurobiol. 114, 102–131.
Carera, E., Tononi, G., 2014. Diaschisis: past, present, future. Brain 137, 2408–2422.
Chou, Y.H., Panych, L.P., Dickey, C.C., Petrella, J.R., Chen, N.K., 2012. Investigation of long-term reproducibility of intrinsic connectivity network mapping: a resting-state fMRI study. Am. J. Neuroradiol. 33, 833–838.
Corbetta, M., Ramsey, L., Callejas, A., Baldassare, A., Hacker, C.D., Siegel, J.S., Astafiev, S.V., Rengachary, J., Zinn, K., Lang, C.E., Tabor Connor, L., Fucetola, R., Strube, M., Carter, A.R., Schulman, G.L., 2015. Common behavioral clusters and subcortical anatomy in stroke. Neuron 85, 927–941.
Crossley, N.A., Mechelli, A., Vértes, P.E., Winton-Brown, T.T., Patel, A.X., Ginestet, C.E., McGuire, P., Bullmore, E.T., 2013. Cognitive relevance of the community structure of the human brain functional coactivation network. PNAS 110, 11583–11588.
Daffertshofer, A., van Wijk, B.C., 2011. On the influence of amplitude on the connectivity between phases. Front. Neuroinform. 5, 6. http://dx.doi.org/10.3389/fninf.2011.00006.
Deco, G., Jirsa, V., McIntosh, A.R., Sporns, O., Kötter, R., 2009. Key role of coupling, delay, and noise in resting brain fluctuations. PNAS 106, 10302–10307.

Deco, G., Jirsa, V.K., McIntosh, A.R., 2013. Resting brains never rest: computational insights into potential cognitive architectures. Trends Neurosci. 36, 268–274.
Deco, G., McIntosh, A.R., Shen, K., Hutchison, R.M., Menon, R.S., Everling, S., Hagmann, P., Jirsa, V.K., 2014. Identification of optimal structural connectivity using functional connectivity and neural modeling. J. Neurosci. 34, 7910–7916.
Faisal, A.A., Selen, L.P.J., Wolpert, D.M., 2008. Noise in the nervous system. Nat. Rev. Neurosci. 9, 292–303.
Freyer, F., Roberts, J.A., Becker, R., Robinson, P.A., Ritter, P., Breakspear, M., 2011. Biophysical mechanisms of multistability in resting-state cortical rhythms. J. Neurosci. 31, 6353–6361.
Freyer, F., Roberts, J.A., Ritter, P., Breakspear, M., 2012. A canonical model of multistability and scale-invariance in biological systems. PLoS Comput. Biol. 8, e1002634. http://dx.doi.org/10.1371/journal.pcbi.1002634.
Fries, P., 2005. A mechanism for cognitive dynamics: neuronal communication through neuronal coherence. Trends Cogn. Sci. 9, 474–480.
Friston, K.J., 2001. The labile brain. I. Neuronal transients and nonlinear coupling. Philos. Trans. R. Soc. B 355, 215–236.
Gamboa, O.L., Tagliazucchi, E., von Wegner, F., Jurcoane, A., Wahl, M., Laufs, H., Ziemann, U., 2014. Working memory performance of early MS patients correlates inversely with modularity increases in resting state functional connectivity networks. NeuroImage 94, 385–395.
Ghosh, A., Rho, Y., McIntosh, A.R., Kötter, R., Jirsa, V.K., 2008. Noise during rest enables the exploration of the brain's dynamic repertoire. PLoS Comput. Biol. 4, e1000196.
Gollo, L.L., Zalesky, A., Hutchison, R.M., van den Heuvel, M., Breakspear, M., 2015. Dwelling quietly in the rich club: brain network determinants of slow cortical fluctuations. Philos. Trans. R. Soc. B 370, 20140165.
Gratton, C., Nomura, E.M., Perez, F., D'Esposito, M., 2012. Focal brain lesions to critical locations cause widespread disruption of the modular organization of the brain. J. Cogn. Neurosci. 24 (6), 1275–1285.
Guimera, R., Amaral, L.A.N., 2005. Functional cartograohy of complex metabolic networks. Nature 433, 895–900.
Hagmann, P., 2005. From Diffusion MRI to Brain Connectomics (PhD Thesis). Ecole Polytechnique Federale de Lausanne, Lausanne.
Hagmann, P., Kurant, J., Gigandet, X., Reto, M., Thiran, J.P., et al., 2007. Mapping human whole-brain structural networks with diffusion MRI. PLoS ONE 2 (7), e597.
Hagmann, P., Cammoun, L., Gigandet, X., Meuli, R., Honey, C.J., et al., 2008. Mapping the structural core of human cerebral cortex. PLoS Biol. 6, e159.
Haimovici, A., Tagliazucchi, E., Balenzuela, P., Chialvo, D.R., 2013. Brain organization into resting state networks emerges at criticality on a model of the human connectome. Phys. Rev. Lett. 110, 178101.
Hansen, E.C.A., Battaglia, D., Spiegler, A., Deco, G., Jirsa, V.K., 2015. Functional connectivity dynamics: modeling the switching behavior of the resting state. NeuroImage 105, 525–535.
Hellyer, P.J., Shanahan, M., Scott, G., Wise, R.J.S., Sharp, D.J., Leech, R., 2014. The control of global brain dynamics: opposing actions of fronto-parietal control and default mode networks on attention. J. Neurosci. 34 (2), 451–461.
Honey, C.J., Sporns, O., 2008. Dynamical consequences of lesions in cortical networks. Hum. Brain Mapp. 29, 802–809.
Honey, C.J., Sporns, O., Cammoun, L., Gigandet, X., Thiran, J.P., et al., 2009. Predicting human resting-state functional connectivity from structural connectivity. PNAS 106, 2035–2040.
Irimia, A., Van Horn, J.D., 2014. Systematic network lesioning reveals the core white matter scaffold of the human brain. Front. Hum. Neurosci. 8, 51. http://dx.doi.org/10.3389/fnhum.2014.00051.
Jones, D.T., Vemuri, P., Murphy, M.C., Gunter, J.L., Senjem, M.L., Machulda, M.M., Przybelski, S.A., Gregg, B.E., Kantarci, K., Knopman, D.S., Boeve, B.F., Petersen, R.C., Jack Jr., C.R., 2012. Non-stationarity in the "resting brain's" modular architecture. PLoS ONE 7, e39731.
Kaiser, M., Martin, R., Andras, P., Young, M.P., 2007. Simulation of robustness against lesions of cortical networks. Eur. J. Neurosci. 25, 3185–3192.
Kelso, J.A.S., 2012. Multistability and metastability: understanding dynamic coordination in the brain. Philos. Trans. R. Soc. Lond. B 367, 906–918.
Kitzbichler, M.G., Smith, M.L., Christensen, S.R., Bullmore, E., 2009. Broadband criticality of human brain network synchronization. PLoS Comput. Biol. 5, e1000314.
Kuramoto, Y., 1984. Chemical Oscillations, Waves and Turbulence. Springer Verlag, New York.
Leech, R., Braga, R., Sharp, D.J., 2012. Echoes of the Brain within the Posterior Cingulate Cortex. J. Neurosci. 32 (1), 215–222.
Lohmann, G., Margulies, D.S., Horstmann, A., Pleger, B., Lepsien, J., Goldhahn, D., Schloegl, H., Stumvoll, M., Villringer, A., Turner, R., 2010. Eigenvector centrality mapping for analyzing connectivity patterns in fMRI data of the human brain. PLoS ONE 5 (4), e10232.
Messé, A., Rudrauf, D., Benali, H., Marrelec, G., 2014. Relating structure and function in the human brain: relative contributions of anatomy, stationary dynamics, and non-stationarities. PLoS Comput. Biol. 10, e1003530.
Meunier, D., Lambiotte, R., Bullmore, E.T., 2010. Modular and hierarchically modular organization of brain networks. Front. Neurosci. 4, 200. http://dx.doi.org/10.3389/fnins.2010.00200.
Meunier, D., Fonlupt, P., Saive, A.-L., Plailly, J., Ravel, N., Royet, J.-P., 2014. Modular structure of functional networks in olfactory memory. NeuroImage 95, 264–275.
Newman, M., 2010. Networks: An Introduction. Oxford University Press, Oxford.
Nir, Y., Fisch, L., Mukamel, R., Gelbard-Sagiv, H., Arielli, A., Fried, I., Malach, R., 2007. Coupling between neuronal firing rate, gamma LFP, and BOLD fMRI is related to interneuronal correlations. Curr. Biol. 17, 1275–1285.
Pendse, G.V., Borsook, D., Becerra, L., 2011. A simple and objective method for reproducible resting state network (RSN) detection in fMRI. PLoS One 6, e27594.
Pikovsky, A., Rosenblum, M., Kurths, J., 2001. Synchronization: A Universal Concept in Nonlinear Sciences. Cambridge University Press, Cambridge.
Platen, E., 1999. An introduction to numerical methods for stochastic differential equations. Acta Numerica 8, 197–246.
Ponce-Alvarez, A., Deco, G., Hagmann, P., Romani, G.L., Mantini, D., Corbetta, M., 2015. Resting-state temporal synchronization networks emerge from connectivity topology and heterogeneity. PLoS Comput. Biol. e1004100.
Rubinov, M., Sporns, O., 2010. Complex network measures of brain connectivity: uses and interpretations. NeuroImage 52, 1059–1069.
Samu, D., Seth, A.K., Nowotny, T., 2014. Influence of wiring cost on the large-scale architecture of human cortical connectivity. PLoS Comput. Biol. 10, e1003557.
Santarnecchi, E., Rossi, S., Rossi, A., 2015. The smarter, the stronger: intelligence level correlates with brain resilience to systematic insults. Cortex 64, 293–309.
Senden, M., Deco, G., de Reus, M.A., Goebel, R., van den Heuvel, M.P., 2014. Rich club organization supports a diverse set of functional network configurations. NeuroImage 96, 174–182.
Shanahan, M., 2010. Metastable chimera states in community-structured oscillator networks. Chaos 20, 013108.
Shanahan, M., 2012. The brain's connective core and its role in animal cognition. Philos. Trans. R. Soc. B 367, 2704–2714.
Smith, S.M., Fox, P.T., Miller, K.L., Glahn, D.C., Fox, P.M., Mackay, C.E., Filippini, N., Watkins, K.E., Toro, R., Laird, A.R., Beckmann, C.F., 2009. Correspondence of the brain's functional architecture during activation and rest. PNAS 106, 13040–13045.
Sporns, O., Tononi, G., Kötter, R., 2005. The human connectome: a structural description of the human brain. PLoS Comput. Biol. 1, e42.
Sporns, O., Honey, C.J., Kötter, R., 2007. Identification and classification of hubs in brain networks. PLoS One 2 (10) e1049.
Tewarie, P., Hillebrand, A., van Dellen, E., Schoonheim, M.M., Barkhof, F., Polman, C.H., Beaulieu, C., Gong, G., van Dijk, B.W., Stam, C.J., 2014. Structural degree predicts functional network connectivity: a multimodal resting-state fMRI and MEG study. NeuroImage 97, 296–307.
Tognoli, E., Kelso, J.A.S., 2014. The metastable brain. Neuron 81, 35–48.
van Dellen, E., Douw, L., Hillebrand, A., Ris-Hilgersom, I.H.M., Schoonheim, M.M., Baayen, J.C., De Witt Hamer, P.C., Velis, D.N., Klein, M., Heimans, J.J., Stam, C.J., Reijneveld, J.C., 2012. MEG network differences between low- and high-grade glioma related to epilepsy and cognition. PLoS ONE 7, e50122.
van Dellen, E., Hillebrand, A., Douw, L., Heimans, J.J., Reijneveld, J.C., Stam, C.J., 2013. Local polymorphic delta activity in cortical lesions causes global decreases in functional connectivity. NeuroImage 83, 524–532.
van den Heuvel, M.P., Sporns, O., 2011. Rich-club organization of the human connectome. J. Neurosci. 31 (44), 15775–15786.
van den Heuvel, M.P., Sporns, O., 2013. An anatomical substrate for integration among functional networks in human cortex. J. Neurosci. 33 (36), 14489–14500.
van den Heuvel, M.P., Kahn, R.S., Goni, J., Sporns, O., 2012. High-cost, high-capacity backbone for global brain communication. PNAS 109 (28), 11372–11377.
Villegas, P., Moretti, P., Muñoz, M.A., 2014. Frustrated hierarchical synchronization and emergent complexity in the human connectome network. Sci. Rep. 4.
Vuksanovic, V., Hövel, P., 2014. Functional connectivity of distant cortical regions: role of remote synchronization and symmetry in interactions. NeuroImage 97, 1–8.
Warren, D.E., Power, J.D., Brussa, J., Denburg, N.L., Waldron, E.J., Sun, H., Petersen, S.E., Tranela, D., 2014. Network measures predict neuropsychological outcome after brain injury. PNAS 111 (39), 14247–14252.
Waxman, S.G., 2006. Axonal conduction and injury in multiple sclerosis: the role of sodium channels. Nat. Rev. Neurosci. 7, 932–941.
Wildie, M., Shanahan, M., 2012. Metastability and chimera states in modular delay and pulse-coupled oscillator networks. Chaos 22, 043131.
You, X., Norr, M., Murphy, E., Kuschner, E.S., Bal, E., Gaillard, W.D., Kenworthy, L., Vaidya, C.J., 2013. Atypical modulation of distant functional connectivity by cognitive state in children with Autism Spectrum Disorders. Front. Hum. Neurosci. 7, 482. http://dx.doi.org/10.3389/fnhum.2013.00482.
Zalesky, A., Fornito, A., Cocchi, L., Gollo, L.L., Breakspear, M., 2014. Time-resolved resting-state brain networks. PNAS 111 (28), 10341–10346.
Zheng, Z., Gang, H., Bambi, H., 1998. Phase slips and phase synchronization of coupled oscillators. Phys. Rev. Lett. 81 (24), 5318–5321.
Zheng, Z., Bambi, H., Gang, H., 2000. Collective phase slips and phase synchronizations in coupled oscillator systems. Phys. Rev. E 62 (1), 402–408.